CHAPTER 40
CAM MECHANISMS

Andrzej A. Olędzki, D.Sc.[†]
Warsaw Technical University, Poland

SUMMARY

This chapter addresses the design of cam systems in which flexibility is not a consideration. Flexible, high-speed cam systems are too involved for handbook presentation. Therefore only two generic families of motion, trigonometric and polynomial, are discussed. This covers most of the practical problems.

The rules concerning the reciprocating motion of a follower can be adapted to angular motion as well as to three-dimensional cams. Some material concerns circular-arc cams, which are still used in some fine mechanisms. In Sec. 40.3 the equations necessary in establishing basic parameters of the cam are given, and the important problem of accuracy is discussed. Force and torque analysis, return springs, and contact stresses are briefly presented in Secs. 40.4 and 40.5, respectively.

The chapter closes with the logic associated with cam design to assist in creating a computer-aided cam design program.

40.1 CAM MECHANISM TYPES, CHARACTERISTICS, AND MOTIONS

Cam-and-follower mechanisms, as linkages, can be divided into two basic groups:

1. Planar cam mechanisms
2. Spatial cam mechanisms

In a planar cam mechanism, all the points of the moving links describe paths in parallel planes. In a spatial mechanism, that requirement is not fulfilled. The design of mechanisms in the two groups has much in common. Thus the fundamentals of planar cam mechanism design can be easily applied to spatial cam mechanisms, which

[†] Prepared while the author was Visiting Professor of Mechanical Engineering, Iowa State University, Ames, Iowa.

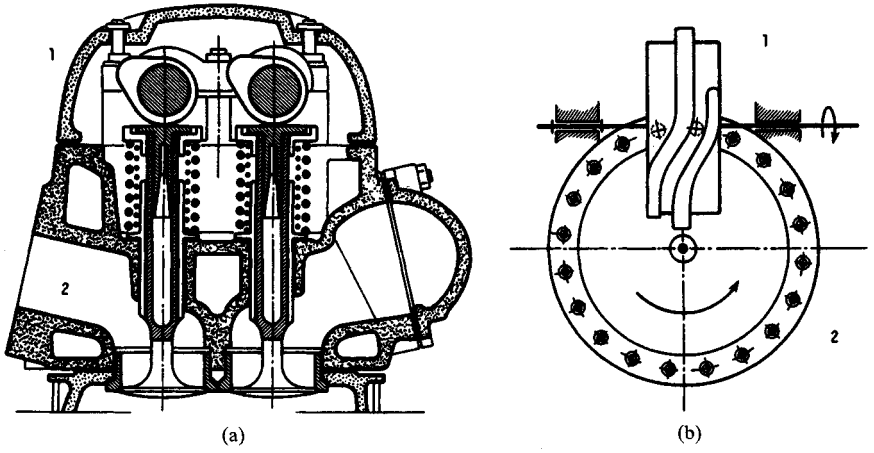

FIGURE 40.1 (*a*) Planar cam mechanism of the internal-combustion-engine D-R-D-R type; (*b*) spatial cam mechanism of the 16-mm film projector R-D-R type.

is not the case in linkages. Examples of planar and spatial mechanisms are depicted in Fig. 40.1.

Planar cam systems may be classified in four ways: (1) according to the motion of the follower—reciprocating or oscillating; (2) in terms of the kind of follower surface in contact—for example, knife-edged, flat-faced, curved-shoe, or roller; (3) in terms of the follower motion—such as dwell-rise-dwell-return (D-R-D-R), dwell-rise-return (D-R-R), rise-return-rise (R-R-R), or rise-dwell-rise (R-D-R); and (4) in terms of the constraining of the follower—spring loading (Fig. 40.1*a*) or positive drive (Fig. 40.1*b*).

Plate cams acting with four different reciprocating followers are depicted in Fig. 40.2 and with oscillating followers in Fig. 40.3.

Further classification of reciprocating followers distinguishes whether the centerline of the follower stem is radial, as in Fig. 40.2, or offset, as in Fig. 40.4.

Flexibility of the actual cam systems requires, in addition to the operating speed, some data concerning the dynamic properties of components in order to find discrepancies between rigid and deformable systems. Such data can be obtained from dynamic models. Almost every actual cam system can, with certain simplifications, be modeled by a one-degree-of-freedom system, shown in Fig. 40.5, where m_e

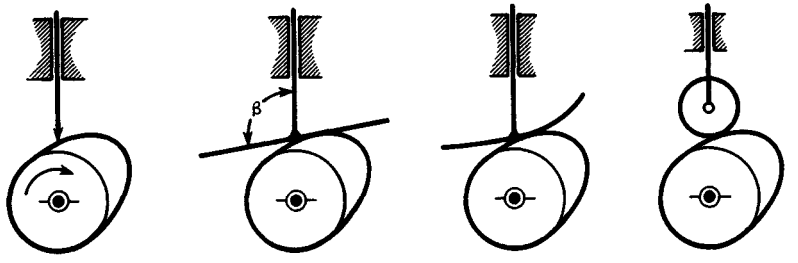

FIGURE 40.2 Plate cams with reciprocating followers.

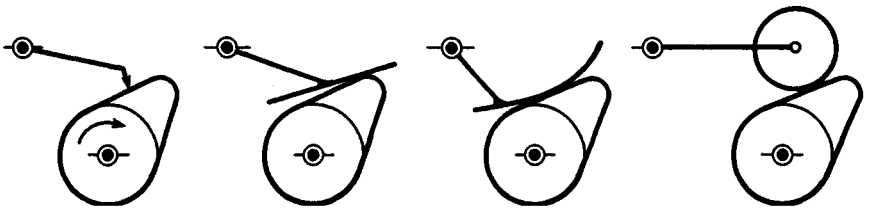

FIGURE 40.3 Plate cams with oscillating followers.

denotes an equivalent mass of the system, k_e equals equivalent stiffness, and s and y denote, respectively, the input (coming from the shape of the cam profile) and the output of the system. The equivalent mass m_e of the system can be calculated from the following equation, based on the assumption that the kinetic energy of that mass equals the kinetic energy of all the links of the mechanism:

$$m_e = \sum_{i=1}^{i=n} \frac{m_i v_i^2}{\dot{s}^2} + \sum_{i=1}^{i=n} \frac{I_i \omega_i^2}{\dot{s}^2}$$

where m_i = mass of link i
v_i = linear velocity of center of mass of ith link
I_i = moment of inertia about center of mass for ith link
ω_i = angular velocity of ith link
$\dot{s}$ = input velocity

The equivalent stiffness k_e can be found from direct measurements of the actual system (after a known force is applied to the last link in the kinematic chain and the displacement of that link is measured), and/or by assuming that k_e equals the actual stiffness of the most flexible link in the chain. In the latter case, k_e can usually be calculated from data from the drawing, since the most flexible links usually have a simple form (for example, a push rod in the automotive cam of Fig. 40.16*c*). In such a

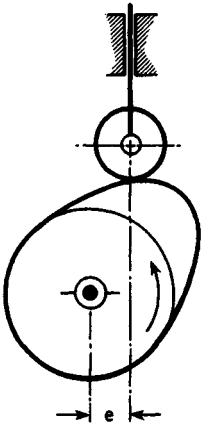

FIGURE 40.4 Plate cam with an offset reciprocating roller follower.

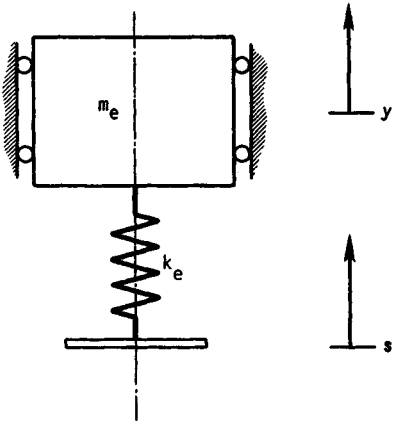

FIGURE 40.5 The one-degree-of-freedom cam system model.

model, the natural frequency of the mass m_e is $\omega_e = \sqrt{k_e/m_e}$ and should be equal to the fundamental frequency ω_n of the actual system.

The motion of the equivalent mass can be described by the differential equation

$$m_e\ddot{y} + k_e(y - s) = 0 \tag{40.1}$$

where $\ddot{y}$ denotes acceleration of the mass m_e. Velocity $\dot{s}$ and acceleration $\ddot{s}$ at the input to the system are

$$\dot{s} = \frac{ds}{dt} = \frac{ds}{d\theta}\frac{d\theta}{dt} = s'\omega \tag{40.2}$$

and

$$\ddot{s} = \frac{d}{dt}s'\omega = ds'\ \omega + s'\frac{d\omega}{dt} = ds'\frac{d\theta}{dt}\omega + s'\alpha$$

$$= s''\omega^2 + s'\alpha \tag{40.3}$$

where θ = angular displacement of cam
α = angular acceleration of cam
$s' = ds/d\theta$, the *geometric velocity*
$s'' = ds'/d\theta = d^2s/d\theta^2$, the *geometric acceleration*

When the cam operates at constant nominal speed $\omega = \omega_0$, $d\omega/dt = \alpha = 0$ and Eq. (40.3) simplifies to

$$\ddot{s} = s''\omega_0^2 \tag{40.4}$$

The same expressions can be used for the actual velocity $\dot{y}$ and for the actual acceleration $\ddot{y}$ at the output of the system. Therefore

$$\dot{y} = y'\omega \tag{40.5}$$

$$\ddot{y} = y''\omega^2 + y'\alpha \tag{40.6}$$

or

$$\ddot{y} = y''\omega_0^2 \qquad \omega = \omega_0 = \text{constant} \tag{40.7}$$

Substituting Eq. (40.7) into Eq. (40.1) and dividing by k_e gives

$$\mu_d y'' + y = s \tag{40.8}$$

where $\mu_d = (m_e/k_e)\omega_0^2$, the *dynamic factor* of the system.

Tesar and Matthew [40.10] classify cam systems by values of μ_d, and their recommendations for the cam designers, depending on the value of μ_d, are as follows:

$\mu_d \cong 10^{-6}$ (for low-speed systems; assume $s = y$)

$\mu_d \cong 10^{-4}$ (for medium-speed systems; use trigonometric, trapezoidal motion specifications, and/or similar ones; synthesize cam at design speed $\omega = \omega_0$, use good manufacturing practices and investigate distortion due to off-speed operations)

$\mu_d \cong 10^{-2}$ (for high-speed systems; use polynomial motion specification and best available manufacturing techniques)

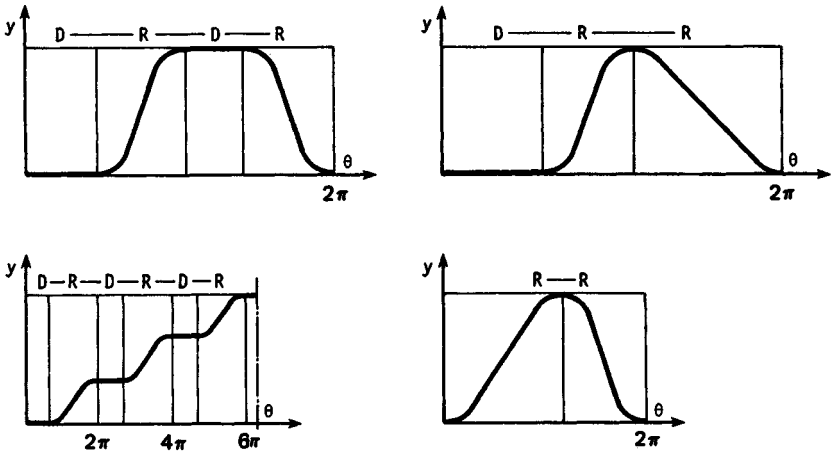

FIGURE 40.6 Types of follower motion.

In all the cases, increasing k_e and reducing m_e are recommended, because it reduces μ_d.

There are two basic phases of the follower motion, *rise* and *return*. They can be combined in different ways, giving types of cams classifiable in terms of the type of follower motion, as in Fig. 40.6.

For positive drives, the symmetric acceleration curves are to be recommended. For cam systems with spring restraint, it is advisable to use unsymmetric curves because they allow smaller springs. Acceleration curves of both the symmetric and unsymmetric types are depicted in Fig. 40.7.

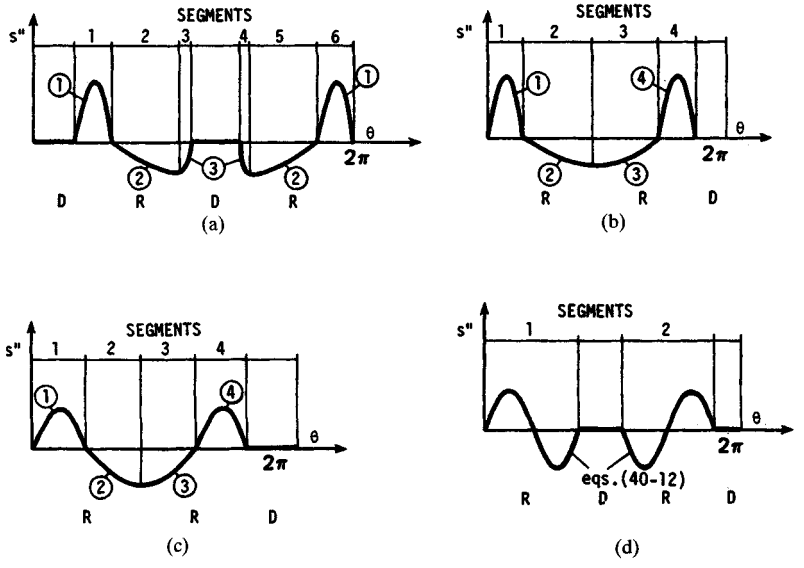

FIGURE 40.7 Acceleration diagrams: (*a*), (*b*) spring loading; (*c*), (*d*) positive drive.

40.2 BASIC CAM MOTIONS

Basic cam motions consist of two families: the trigonometric and the polynomial.

40.2.1 Trigonometric Family

This family is of the form

$$s'' = C_0 + C_1 \sin a\theta + C_2 \cos b\theta \tag{40.9}$$

where C_0, C_1, a, and b are constants.

For the low-speed systems where $\mu_d < 10^{-4}$, we can construct all the necessary diagrams, symmetric and unsymmetric, from just two curves: a sine curve and a cosine curve.

Assuming that the total rise or return motion s_0 occurs for an angular displacement of the cam $\theta = \beta_0$, we can partition acceleration curves into i separate segments, where $i = 1, 2, 3, \ldots$ with subtended angles $\beta_1, \beta_2, \beta_3, \ldots$ so that $\beta_1 + \beta_2 + \beta_3 + \cdots = \beta_0$. The sum of partial lifts $s_1, s_2, s_3, \ldots$ in the separate segments should be equal to the total rise or return s_0: $s_1 + s_2 + s_3 + \cdots = s_0$. If a dimensionless description θ/β of cam rotation is introduced into a segment, we will have the value of ratio θ/β equal to zero at the beginning of each segment and equal to unity at the end of each segment.

All the separate segments of the acceleration curves can be described by equations of the kind

$$s'' = A \sin \frac{n\pi\theta}{\beta} \qquad n = \frac{1}{2}, 1, 2 \tag{40.10}$$

or

$$s'' = A \cos \frac{\pi\theta}{2\beta} \tag{40.11}$$

where A is the maximum or minimum value of the acceleration in the individual segment.

The simplest case is when we have a positive drive with a symmetric acceleration curve (Fig. 40.7*d*). The complete rise motion can be described by a set of equations

$$\begin{aligned} s &= s_0 \left(\frac{\theta}{\beta} - \frac{1}{2\pi} \sin \frac{2\pi\theta}{\beta} \right) & s'' &= \frac{2\pi s_0}{\beta^2} \sin \frac{2\pi\theta}{\beta} \\ s' &= \frac{s_0}{\beta} \left(1 - \cos \frac{2\pi\theta}{\beta} \right) & s''' &= \frac{4\pi^2 s_0}{\beta^3} \cos \frac{2\pi\theta}{\beta} \end{aligned} \tag{40.12}$$

The last term is called *geometric jerk* ($\dddot{s} = \omega^3 s'''$). Traditionally, this motion is called *cycloidal.*

The same equations can be used for the return motion of the follower. It is easy to prove that

$$\begin{aligned} s_{\text{return}} &= s_0 - s_{\text{rise}} & s''_{\text{return}} &= -s''_{\text{rise}} \\ s'_{\text{return}} &= -s'_{\text{rise}} & s'''_{\text{return}} &= -s'''_{\text{rise}} \end{aligned} \tag{40.13}$$

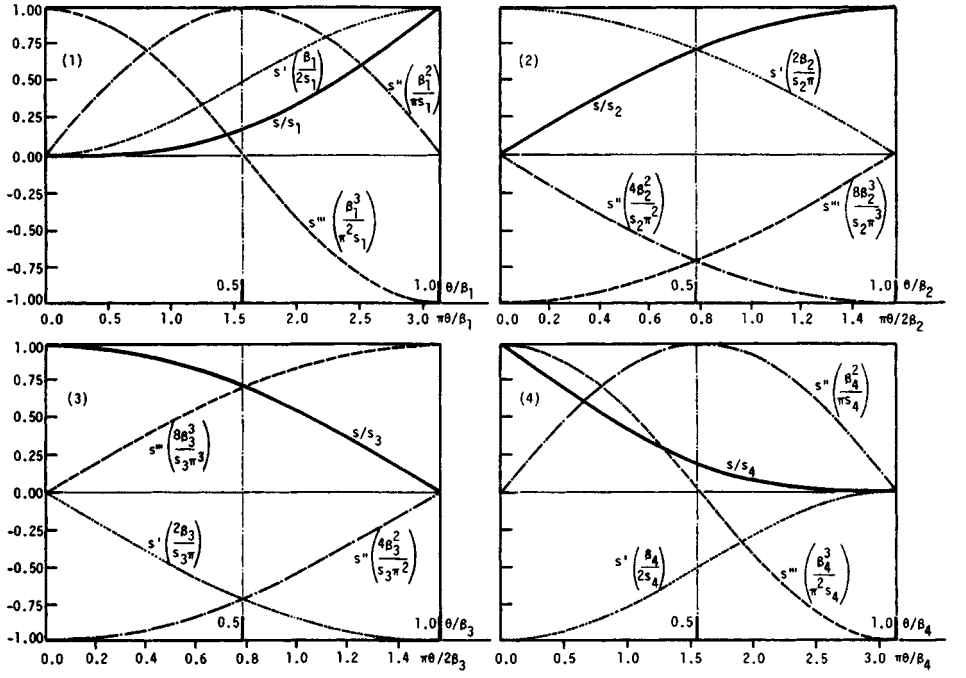

FIGURE 40.8 Trigonometric standard follower motions (according to the equation of Table 40.1, for $c = d = 0$).

All the other acceleration curves, symmetric and unsymmetric, can be constructed from just four trigonometric standard follower motions. They are denoted further by the numbers 1 through 4 (Fig. 40.8). These are displayed in Table 40.1.

Equations in Table 40.1 can be used to represent the different segments of a follower's displacement diagram. Derivatives of displacement diagrams for the adjacent segments should match each other; thus several requirements must be met in order to splice them together to form the motion specification for a complete cam. Motions 1 through 4 have the following applications:

Motion 1 is for the initial part of a rise motion.

Motion 2 is for the end and/or the middle part of a rise motion and the initial part of a return motion. The value c is a constant, equal to zero only in application to the end part of a rise motion.

Motion 3 is for the end part of a rise motion and/or the initial or middle part of a return motion. The value d is a constant, equal to zero only in application to the initial part of a return motion.

Motion 4 is for the end part of a return motion.

The procedure of matching the adjacent segments is best understood through examples.

Example 1. This is an extended version of Example 5-2 from Shigley and Uicker [40.8], p. 229. Determine the motion specifications of a plate cam with reciprocating

TABLE 40.1 Standard Trigonometric Follower Motions

Parameter	Motion 1	Motion 2	Motion 3	Motion 4
s	$\frac{s_1}{\pi}\left(\frac{\pi\theta}{\beta_1} - \sin\frac{\pi\theta}{\beta_1}\right)$	$s_2 \sin\frac{\pi\theta}{2\beta_2} + c\frac{\theta}{\beta_2}$	$s_3 \cos\frac{\pi\theta}{2\beta_3} + d\left(\frac{\theta}{\beta_3} - \frac{1}{2}\right)$	$s_4\left(1 - \frac{\theta}{\beta_4} - \frac{1}{\pi}\sin\frac{\pi\theta}{\beta_4}\right)$
s'	$\frac{s_1}{\beta_1}\left(1 - \cos\frac{\pi\theta}{\beta_1}\right)$	$\frac{s_2\pi}{2\beta_2}\cos\frac{\pi\theta}{2\beta_2} + \frac{c}{\beta_2}$	$-\frac{s_3\pi}{2\beta_3}\sin\frac{\pi\theta}{2\beta_3} + \frac{d}{\beta_3}$	$-\frac{s_4}{\beta_4}\left(1 + \cos\frac{\pi\theta}{\beta_4}\right)$
s''	$\frac{\pi s_1}{\beta_1^2}\sin\frac{\pi\theta}{\beta_1}$	$-\frac{s_2\pi^2}{4\beta_2^2}\sin\frac{\pi\theta}{2\beta_2}$	$-\frac{s_3\pi^2}{4\beta_3^2}\cos\frac{\pi\theta}{2\beta_3}$	$\frac{\pi s_4}{\beta_4^2}\sin\frac{\pi\theta}{\beta_4}$
s'''	$\frac{\pi^2 s_1}{\beta_1^3}\cos\frac{\pi\theta}{\beta_1}$	$-\frac{s_2\pi^3}{8\beta_2^3}\cos\frac{\pi\theta}{2\beta_2}$	$\frac{s_3\pi^3}{8\beta_3^3}\sin\frac{\pi\theta}{2\beta_3}$	$\frac{\pi^2 s_4}{\beta_4^3}\cos\frac{\pi\theta}{\beta_4}$
$s'_{i,\ \text{init}}\left(\frac{\theta}{\beta_i} = 0\right)$	. . .	$\frac{s_2\pi}{2\beta_2}$	$\frac{d}{\beta_3}$	$-\frac{2s_4}{\beta_4}$
$s'_{i,\ \text{end}}\left(\frac{\theta}{\beta_i} = 1\right)$	$\frac{2s_1}{\beta_1}$	$\frac{c}{\beta_2}$	$-\frac{s_3\pi}{2\beta_3} + \frac{d}{\beta_3}$	
$s''_{\max}$; $s''_{\min}$	$s''_{\max} = \frac{\pi s_1}{\beta_1^2}$	$s''_{\min} = -\frac{s_2\pi^2}{4\beta_2^2}$	$s''_{\min} - \frac{s_3\pi^2}{4\beta_3^2}$	$s''_{\max} = \frac{\pi s_4}{\beta_4^2}$

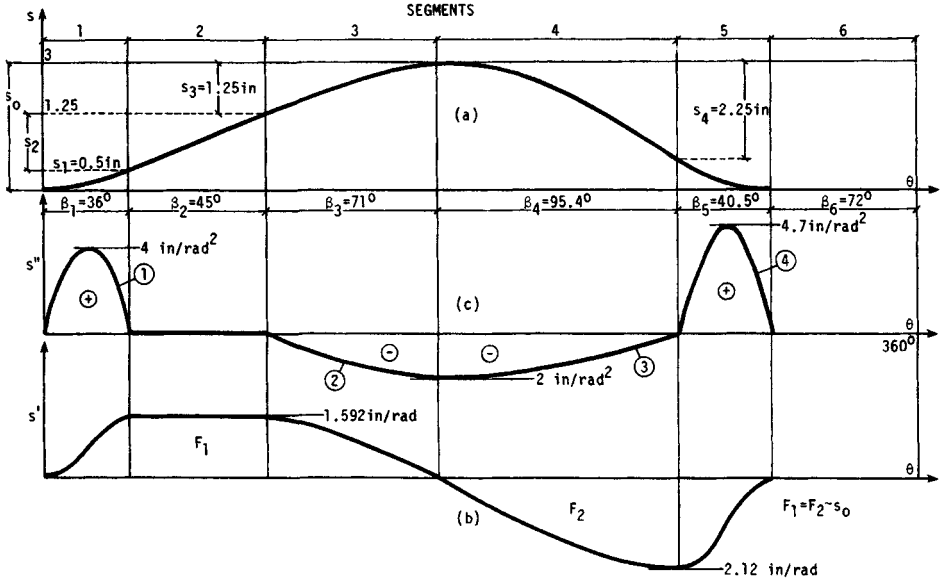

FIGURE 40.9 Example 1: (*a*) displacement diagram, in; (*b*) geometric velocity diagram, in/rad; (*c*) geometric acceleration diagram, in/rad².

follower and return spring for the following requirements: The speed of the cam is constant and equal to 150 r/min. Motion of the follower consists of six segments (Fig. 40.9):

1. Accelerated motion to $\dot{s}_{1,\text{end}} = 25$ in/s (0.635 m/s)
2. Motion with constant velocity 25 in/s, lasting for 1.25 in (0.03175 m) of rise
3. Decelerated motion (segments 1 to 3 describe rise of the follower)
4. Return motion
5. Return motion
6. Dwell, lasting for $t \geq 0.085$ s

The total lift of the follower is 3 in (0.0762 m).

Solution. Angular velocity $\omega = 150\pi/30 = 15.708$ radians per second (rad/s). The cam rotation for 1.25 in of rise is equal to $\beta_2 = 1.25$ in/$s_2' = 1.25$ in/1.592 in/rad = 0.785 rad = 45°, where $s_2' = 25/15.708 = 1.592$ in/rad.

The following decisions are quite arbitrary and depend on the designer:

1. Use motion 1; then $s_1 = 0.5$ in, $s''_{\max} = 0.05\pi/\beta_1^2 = 0.5\pi/(0.628)^2 = 4$ in/rad² (0.1016 m/rad²). $s''_{1,\text{end}} = 2(0.5)/\beta_1$; so $\beta_1 = 1/1.592 = 0.628$ rad, or 36°.
2. For the motion with constant velocity, $s_2' = 1.592$ in/rad (0.4044 m/rad); $s_2 = 1.25$ in.
3. Motion type 2: $s_3 = s_2 = 1.25$ in, $s'_{3,\text{init}} = s_3\pi/(2\beta_3) = 1.592$ in/rad; therefore $\beta_3 = 1.25\pi/[2(1.592)] = 1.233$ rad $\cong 71°$, $s'''_{3,\min} = -(1.25\pi^2)/[4(1.233)^2] = -2$ in/rad². (Points 1 through 3 describe the rise motion of the follower.)
4. Motion type 3: $s''_{4,\text{init}} = s_4\pi^2/(4\beta_r^2) = -2$ in/rad² (the same value as that of $s''_{3,\min}$), $s''_{4,\text{end}} = -\pi s_4/(2\beta_4)$, $s_4 + s_5 = 3$ in.

5. Motion type 4: $s''_{5,\max} = \pi s_5/\beta_5^2$, $s'_{5,\text{init}} = -s'_{4,\text{end}} = -2s_5/\beta_5$. We have here the four unknowns β_4, s_4, β_5, and s_5. Assuming time $t_6 = 0.85$ s for the sixth segment (a dwell), we can find $\beta_6 = \omega t_6 = 15.708(0.08) = 1.2566$ rad, or 72°. Therefore $\beta_4 + \beta_5 = 136°$, or 2.374 rad (Fig. 40.9). Three other equations are $s_4 + s_5 = 3$, $s_4\pi^2/(4\beta_4^2) = 2$, and $\pi s_4/(2\beta_4) = 2s_5/\beta_5$. From these we can derive the quadratic equation in β_4.

$$0.696\beta_4^2 + 6.044\beta_4 - 12 = 0$$

Solving it, we find $\beta_4 = 1.665\ 848$ rad $\cong 95.5°$ and $\beta_5 = 40.5°$. Since $s_4/s_5 = 4\beta_4/(\pi\beta_5) = 3.000\ 76$, it is easy to find that $s_5 = 0.75$ in (0.019 05 m) and $s_4 = 2.25$ in (0.057 15 m). Maximum geometric acceleration for the fifth segment $s''_{5,\max} = 4.7$ in/rad^2 (0.0254 m/rad^2), and the border (matching) geometric velocity $s'_{4,\text{end}} = s'_{5,\text{init}} = 2.12$ in/rad (0.253 m/rad).

Example 2. Now let us consider a cam mechanism with spring loading of the type D-R-D-R (Fig. 40.7*a*). The rise part of the follower motion might be constructed of three segments (1, 2, and 3) described by standard follower motions 1, 2, and 3 (Fig. 40.8). The values of constants c and d in Table 40.1 are no longer zero and should be found from the boundary conditions. (They are zero only in the motion case R-R-D, shown in Fig. 40.7*b*, where there is no dwell between the rise and return motions.)

For a given motion specification for the rise motion, the total follower stroke s_0, and the total angular displacement of the cam β_0, we have eight unknowns: β_1, s_1, β_2, s_2, β_3, s_3, and constants c and d. The requirements of matching the displacement derivatives will give us only six equations; thus two more must be added to get a unique solution. Two additional equations can be written on the basis of two arbitrary decisions:

1. The maximum value of the acceleration in segment 1, $s''_{1,\max}$ should be greater than that in segment 2 because of spring loading. So $s''_{1,\max} = -as''_{2,\min}$ where $s''_{2,\min}$ is the minimum value of the second-segment acceleration and a is any assumed number, usually greater than 2.
2. The end part of the rise (segment 3), the purpose of which is to avoid a sudden drop in a negative accelerative curve, should have a smaller duration than the basic negative part (segment 2). Therefore we can assume any number b (greater than 5) and write $\beta_2 = b\beta_3$. The following formulas were found after all eight equations for the eight unknowns were solved simultaneously:

$$\beta_1 = \frac{\beta_0}{1 + a + a/b} \qquad \beta_3 = \beta_0 \frac{a}{a(1+b) + b}$$

$$s_1 = s_0 \frac{\pi b^2}{b^2(\pi + 4a) + 4a(2a + 1)} \qquad s'_2 = s_1 \frac{4a}{\pi}$$

$$s_3 = s_1 \frac{4a}{\pi b^2} \qquad c = s_1 \frac{8a^2}{\pi b^2}$$

$$d = 2s_3 \qquad s_0 = s_1 + s'_2 + c + s_3$$

We can assume practical values for a and b (say $a = 2, b = 10$) and find from the above equations the set of all the parameters (as functions of s_0 and β_0) necessary to form

the motion specification for the rise motion of the follower and the shape of the cam profile. The whole set of parameters is as follows:

$$s_1 = 0.272\,198 s_0 \qquad \beta_1 = 0.312\,5\beta_0$$

$$s_2' = 0.693\,147 s_0 \qquad c = 0.027\,726 s_0$$

$$\beta_2 = 0.625\beta_0$$

$$s_3 = 0.006\,931 s_0 \qquad d = 2s_3 \quad \text{(always!)}$$

$$\beta_3 = 0.0625\beta_0$$

These can be used for calculations of the table $s = s(\theta)$, which is necessary for manufacturing a cam profile. For such a table, we use as a rule increments of θ equal to about 1° and accuracy of s up to 4×10^{-5} in 1 micrometer (μm). The data of such a table can be easily used for the description of both the return motion of the follower and a cam profile, providing $\beta_0(\text{return}) = \beta_0(\text{rise})$, and the acceleration diagram for the return motion is a mirror image of the acceleration diagram for the rise motion. Table 40.2 can be of assistance in calculating the return portion of the cam profile. The column s(return) is the same as the column s(rise).

TABLE 40.2 Data of Rise Motion Used for Calculations of Return Portion of Cam Profile

Rise		Return	
θ(rise)	s(rise)	θ(return)	s(return)
0	0	$2\beta_0 + \beta_d - 0$	0
⋮	⋮	⋮	⋮
θ_i	s_i	$2\beta_0 + \beta_d - \theta_i$	s_i
⋮	⋮	⋮	⋮
β_0	s_0	$2\beta_0 + \beta_d - \beta_0$	s_0

The trigonometric acceleration diagram for the positive drive was described at the beginning of this section by Eq. (40.12). The improved diagram (smaller maximum values of acceleration for the same values of s_0 and β_0[†]) can be obtained if we combine sine segments with segments of constant acceleration. Such a diagram, called a *modified trapezoidal acceleration curve,* is shown in Fig. 40.10. Segments 1, 3, 4, and 6 are the sinusoidal type. Sections 2 and 5 are with $s'' =$ constant. It was assumed for that diagram that all the sine segments take one-eighth of the total angular displacement β_0 of the cam during its rise motion. The first half of the motion has three segments. The equations for the first segment are $0 \le \theta/\beta_0 \le \frac{1}{8}$, and so

[†] The maximum acceleration ratio is 4.9/6.28.

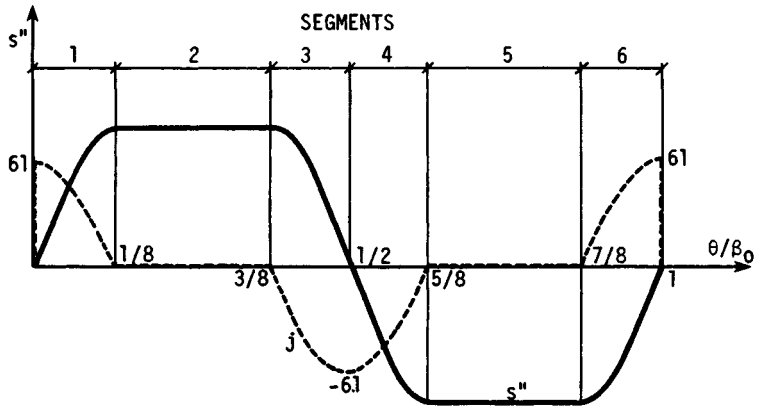

FIGURE 40.10 A modified trapezoidal acceleration diagram.

$$s = \frac{s_0'}{2\pi}\left(\frac{4\pi\theta}{\beta_0} - \sin\frac{4\pi\theta}{\beta_0}\right) \qquad s' = \frac{2s_0'}{\beta_0}\left(1 - \cos\frac{4\pi\theta}{\beta_0}\right)$$

$$s'' = 8\pi\frac{s_0'}{\beta_0^2}\sin\frac{4\pi\theta}{\beta_0} \qquad s''' = 32\pi^2\frac{s_0'}{\beta_0^3}\cos\frac{4\pi\theta}{\beta_0} \tag{40.14}$$

For the second segment, we have $\frac{1}{8} \le \theta/\beta_0 \le \frac{3}{8}$, and so

$$s = s_0'\left[-\frac{1}{2\pi} + \frac{2\theta}{\beta_0} + 4\pi\left(\frac{\theta}{\beta_0} - \frac{1}{8}\right)^2\right]$$

$$s' = \frac{s_0'}{\beta_0}\left[2 + 8\pi\left(\frac{\theta}{\beta_0} - \frac{1}{8}\right)\right] \tag{40.15}$$

$$s'' = \frac{8\pi s_0'}{\beta_0^2} \qquad s''' = 0$$

The relations for the third segment are $\frac{3}{8} \le \theta/\beta_0 \le \frac{5}{8}$ ([40.7]); therefore,

$$s = s_0'\left\{-\frac{\pi}{2} + 2(1+\pi)\frac{\theta}{\beta_0} - \frac{1}{2\pi}\sin\left[4\pi\left(\frac{\theta}{\beta_0} - \frac{2}{8}\right)\right]\right\}$$

$$s' = \frac{2s_0'}{\beta_0}\left\{1 + \pi - \cos\left[4\pi\left(\frac{\theta}{\beta_0} - \frac{2}{8}\right)\right]\right\} \tag{40.16}$$

$$s'' = \frac{8\pi s_0'}{\beta_0^2}\sin\left[4\pi\left(\frac{\theta}{\beta_0} - \frac{2}{8}\right)\right]$$

$$s''' = 32\pi^2\frac{s_0'}{\beta_0^3}\cos\left[4\pi\left(\frac{\theta}{\beta_0} - \frac{2}{8}\right)\right]$$

where $s_0' = s_0/(2 + \pi) = 0.194\,492 s_0$.

Using Eqs. (40.14) through (40.16) for all three segments, we can calculate the s values for the first half of the rise motion, where $\theta/\beta_0 = \frac{1}{8}$ and $s = s_0/2$. Since the negative part of the acceleration diagram is a mirror image of the positive part, it is easy to calculate the s values for the second half of the rise motion from the data obtained for the first half. The necessary procedure for that is shown in Table 40.3. The procedure concerns the case with the modified trapezoidal acceleration diagram, but it could be used as well for all the cases with symmetric acceleration diagrams for the rise motion. For the return motion of the follower, when its acceleration diagram is a mirror image of the rise diagram, we can use again the technique shown in Table 40.2. All the calculations can be done simultaneously by the computer after a simple program is written.

TABLE 40.3 Data of First Half of Rise Motion Used for Calculations of Second Half

		$\gamma = \theta/\beta_o$	s	γ	s	
Segments	1	0 $\vdots$ γ_i $\vdots$ $\frac{1}{8}$	0 $\vdots$ s_i $\vdots$ $s_1 = s_0'(\pi/2 - 1)/2\pi$	1 $\vdots$ $1 - \gamma_i$ $\vdots$ $\frac{7}{8}$	s_0 $\vdots$ $s_0 - s_i$ $\vdots$ $s_0 - s_1$	6
	2	$\frac{1}{8}$ $\vdots$ γ_j $\vdots$ $\frac{3}{8}$	s_1 $\vdots$ s_j $\vdots$ $s_2 = s_0'(\frac{3}{4} - 1/2\pi + \pi/4)$	$\frac{7}{8}$ $\vdots$ $1 - \gamma_j$ $\vdots$ $\frac{5}{8}$	$s_0 - s_1$ $\vdots$ $s_0 - s_j$ $\vdots$ $s_0 - s_2$	5
	3	$\frac{3}{8}$ $\vdots$ γ_k $\vdots$ $\frac{4}{8}$	s_2 $\vdots$ s_k $\vdots$ $s_3 = s_0/2$	$\frac{5}{8}$ $\vdots$ $1 - \gamma_k$ $\vdots$ $\frac{4}{8}$	$s_0 - s_2$ $\vdots$ $s_0 - s_k$ $\vdots$ $s_0 - s_3 = s_0/2$	4

All the trigonometric curves of this section were calculated with finite values of jerk, which is of great importance for the dynamic behavior of the cam mechanism. An example of the jerk diagram is given in Fig. 40.10. The jerk curve j was plotted by using the dimensionless expression

$$j = \frac{s'''}{s_0/\beta_0^3} \tag{40.17}$$

This form of the jerk description can also be used to compare properties of different acceleration diagrams.

40.2.2 Polynomial Family

The basic polynomial equation is

$$s = C_0 + C_1\frac{\theta}{\beta_0} + C_2\left(\frac{\theta}{\beta_0}\right)^2 + C_3\left(\frac{\theta}{\beta_0}\right)^3 + \cdots \tag{40.18}$$

with constants C_i depending on assumed initial and final conditions.

This family is especially useful in the design of flexible cam systems, where values of the dynamic factor are $\mu_d \geq 10^{-2}$. Dudley (1947) first used polynomials for the synthesis of flexible systems, and his ideal later was improved by Stoddart [40.9] in application to automotive cam gears.

The shape factor s of the cam profile can be found by this method after a priori decisions are made about the motion y of the last link in the kinematic chain. Cams of that kind are called *polydyne cams.*

When flexibility of the system can be neglected, the initial and final conditions ([40.3], [40.4], and [40.8]) might be as follows (positive drive):

1. Initial conditions for full-rise motion are

$$\frac{\theta}{\beta_0} = 0 \qquad s = 0 \qquad s' = 0 \qquad s'' = 0$$

2. Final (end) conditions are

$$\frac{\theta}{\beta_0} = 1 \qquad s = s_0 \qquad s' = 0 \qquad s'' = 0$$

The first and second derivatives of Eq. (40.18) are

$$s' = C_1 + 2C_2\frac{\theta}{\beta_0} + 3C_3\left(\frac{\theta}{\beta_0}\right)^2 + 4C_4\left(\frac{\theta}{\beta_0}\right)^3 + \cdots$$

$$s'' = 2C_2 + 6C_3\frac{\theta}{\beta_0} + 12C_4\left(\frac{\theta}{\beta_0}\right)^2 + \cdots \tag{40.19}$$

Substituting six initial and final conditions into Eqs. (40.18) and (40.19) and solving them simultaneously for unknowns C_0, C_1, C_2, C_3, C_4, and C_5, we have

$$s = 10s_0\left[\left(\frac{\theta}{\beta_0}\right)^3 - 1.5\left(\frac{\theta}{\beta_0}\right)^4 + 0.6\left(\frac{\theta}{\beta_0}\right)^5\right]$$

$$s' = 30\frac{s_0}{\beta_0}\left[\left(\frac{\theta}{\beta_0}\right)^2 - 2\left(\frac{\theta}{\beta_0}\right)^3 + \left(\frac{\theta}{\beta_0}\right)^4\right] \tag{40.20}$$

$$s'' = 60\frac{s_0}{\beta_0^2}\left[\frac{\theta}{\beta_0} - 3\left(\frac{\theta}{\beta_0}\right)^2 + 2\left(\frac{\theta}{\beta_0}\right)^3\right]$$

and for a jerk $s''' = ds''/d\theta$, or

$$s''' = 60\frac{s_0}{\beta_0^3}\left[1 - 6\frac{\theta}{\beta_0} + 6\left(\frac{\theta}{\beta_0}\right)^2\right]$$

This is called the polynomial 3-4-5, since powers 3, 4, and 5 remain in the displacement equation. It provides a fairly good diagram for the positive drives.

Equations for the full-return polynomial are

$$\begin{aligned} s(\text{return}) &= -s(\text{rise}) + s_0 & s''(\text{return}) &= -s'(\text{rise}) \\ s''(\text{return}) &= -s''(\text{rise}) & s'''(\text{return}) &= -s'''(\text{rise}) \end{aligned} \tag{40.21}$$

All the characteristic curves of the full-rise 3-4-5 polynomial are shown in Fig. 40.11. They were generated by the computer for $s_0 = 1$ displacement unit (inches or centimeters) and $\beta_0 = 1$ rad.

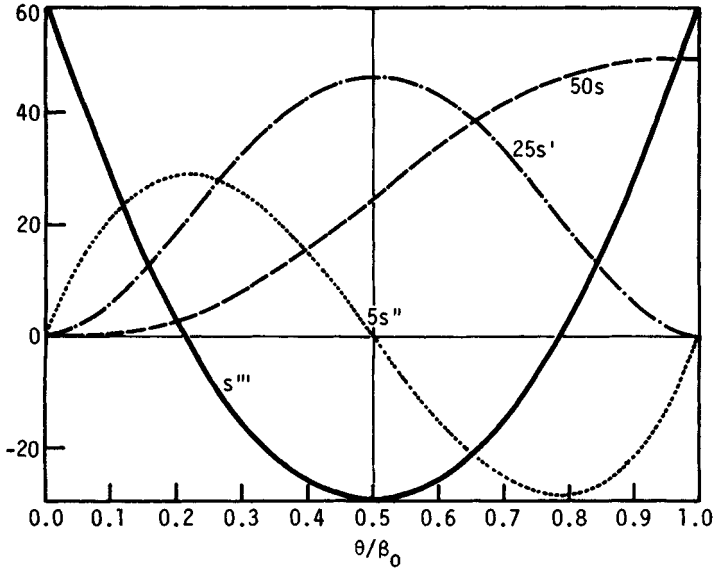

FIGURE 40.11 Full-rise 3-4-5 polynomial motion.

After a proper set of initial and final conditions is established, the basic equation [Eq. (40.18)] can be used for describing any kind of follower motion with an unsymmetric acceleration diagram. Details concerning the necessary procedure can be found in Rothbart [40.7].

40.2.3 Other Cam Motions

The basic cam motions described in the previous sections cover most of the routine needs of the contemporary cam designer. However, sometimes the cost of manufacturing the cam profile may be too high and the dynamic properties of the cam motion may not be severe. This is the case of cams used for generating functions. There is a very effective approach, described by Mischke [40.2], concerning an optimum design of simple eccentric cams. They are very inexpensive, yet can be used even for generating very complicated functions.

The other approach, when we are interested in inexpensive cams, is to use *circular-arc* cams or *tangent* cams. They are still used in low-speed diesel IC engines since the cost of their manufacture is low (compare with Fig. 40.15). An extensive review of these cams can be found in Rothbart [40.7]. They were used quite frequently in the past when the speed of machines was low, but today they are not often recommended because their dynamic characteristics are poor. The only exception can be made for fine- or light-duty mechanisms, such as those of 8- and 16-mm film projectors, where circular-arc cams are still widely used. Those cams are usually of the positive drive kind, where the breadth of the cam is constant. The cam drives a reciprocating follower with two flat working surfaces a fixed distance apart, which contact opposite sides of the cam.

The constant-breadth cam is depicted in Fig. 40.12. For given values of radius ρ, total angle of cam rotation β_0, and total lift of the follower s_0, the basic dimensions of the cam can be found from the relations ([40.11])

$$R_1 = \frac{\rho - b(s_0 + \rho)}{1 - b} \qquad r = R_1 - s_0 \tag{40.22}$$

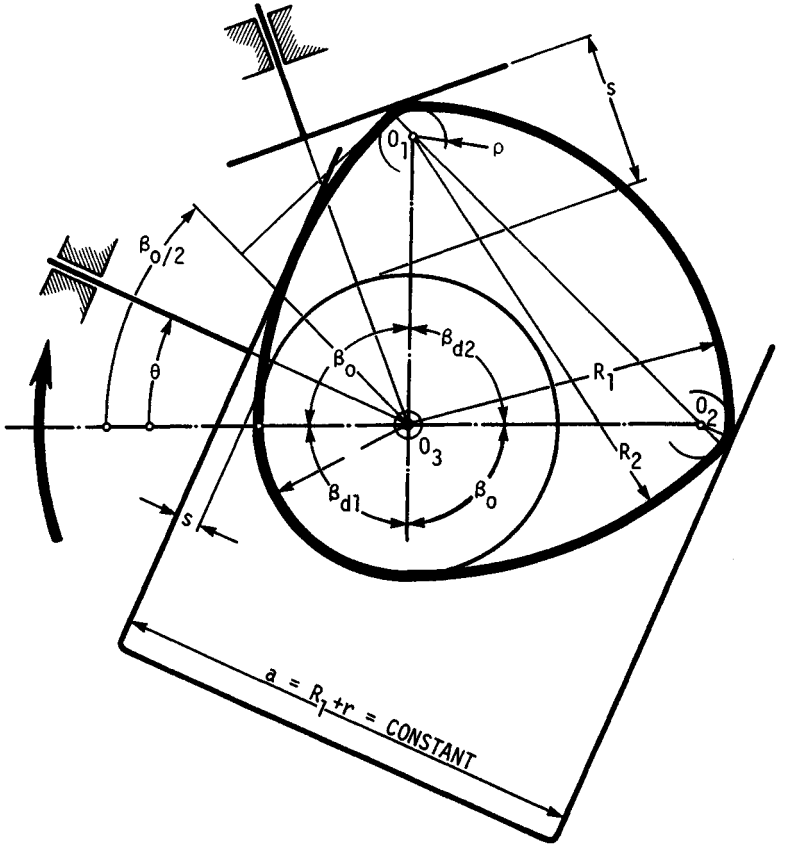

FIGURE 40.12 Constant-breadth circular-arc cam.

where $b = \cos 0.25\beta_0/\cos 0.75\beta_0$. Cam motions for full rise ($0 \geq \theta \geq \beta_0$) are described in Table 40.4. Such cams are symmetric; therefore, β_0(rise) = β_0(return), and the two dwells β_{d1} and β_{d2} are the same and equal to $180° - \beta_0$. Table 40.4 can also be used for calculation of full-return motion. Dimensions of the cam (R_1) and maximum values of the acceleration increase with a decrease in β_0. Acceleration diagrams for different values of β_0 are shown in Fig. 40.13.

TABLE 40.4 Basic Equations for a Constant-Breadth Circular-Arc Cam, Using $A = R_1 - \rho$

Parameter	$0 \leq \theta \leq /\beta_0/2$	$\beta_0/2 \leq \theta \leq \beta_0$
s	$A(1 - \cos\theta)$	$A\cos(\beta_0 - \theta) - (r - \rho)$
s'	$A \sin\theta$	$A \sin(\beta_0 - \theta)$
s''	$A \cos\theta$	$-A \cos(\beta_0 - \theta)$
s'''	$-A \sin\theta$†	$-A \sin(\beta_0 - \theta)$†

† Both equations are valid, however, only inside the partitions. For $\theta = 0, \beta_0/2$, and β_0, $s''' \to \infty$.

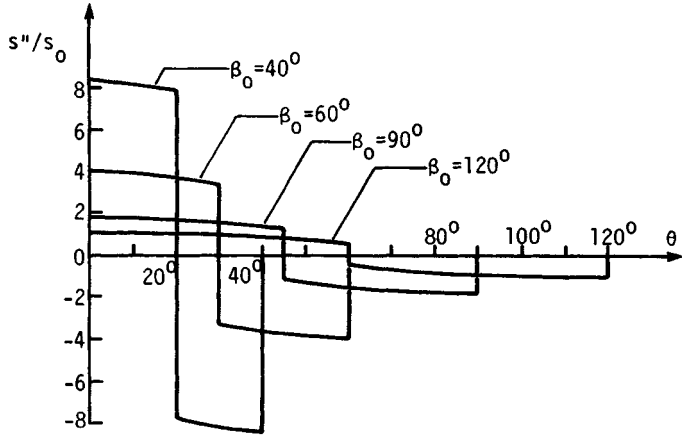

FIGURE 40.13 Acceleration diagrams.

40.3 LAYOUT AND DESIGN; MANUFACTURING CONSIDERATIONS

The cam profile is an inner envelope of the working surface of the follower. After the displacement diagram is determined, the cam layout can be found by using the usual graphical approach or by computer graphics with a rather simple computer program.

In the design of a plate cam with a reciprocating flat-face follower, the geometric parameters necessary for its layout are the prime-circle radius R_0, the minimum

width of the follower face F, and the offset e of the follower face. The value R_0 can be found from

$$R_0 > (\rho_{min} - s'' - s)_{max} \tag{40.23}$$

where ρ_{min} is a minimum value of the radius ρ of the cam-profile curvature. Its value for such practical reasons as contact stresses might be assumed equal to 0.2 to 0.25 in [5 to 6 millimeters (mm)]. Since s is always positive, we should examine that part of the follower acceleration diagram for the rise motion where acceleration is negative.

The face width F can be calculated from

$$F > s'_{max} - s'_{min} \tag{40.24}$$

To avoid undercutting cams with a roller follower, the radius R_r of the roller must always be smaller than $|\rho|$, where ρ is the radius of curvature.

The pressure angle γ (Fig. 40.14) is an angle between a common normal to both the roller and the cam profile and the direction of the follower motion. This angle can be calculated from

$$\tan \gamma = \frac{s'}{s + R_0 + R_r} \tag{40.25}$$

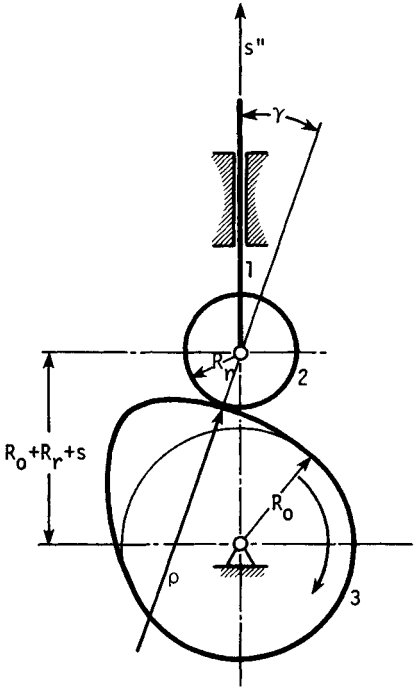

FIGURE 40.14 Cam mechanism with reciprocating roller follower.

It is a common rule of thumb to assume for the preliminary calculation that γ_{max} is not greater than 30° for the reciprocating follower motion (or 45° for the oscillating one). Acceptable values of γ_{max} that can be used without causing difficulties depend, however, on the particular cam mechanism design and should be found for any actual mechanism from the dynamic analysis.

After establishing the value of γ_{max} and R_r in accordance with the preliminary layout of the mechanism, we can find the value of the prime-circle radius R_0 from the equation

$$R_0 \geq \left(\frac{s'}{\tan \gamma_{max}} - s - R_r \right)_{max} \tag{40.26}$$

Now check whether the assumed value of R_r is small enough to avoid undercutting of the cam profile. It can be done ([40.7]) by using Eq. (40.27):

$$R_r \leq \left[\frac{|s'|}{\sin^3 \gamma_{max} \left(\frac{1}{\sin^3 \gamma_{max}} + 2 - \frac{s''}{|s'| \tan \gamma_{max}} - \frac{1}{|s'|} \right)} \right]_{min} - \rho_{min} \tag{40.27}$$

The primary choice of the follower motion should always be guided by a good understanding of the planned manufacturing technique. *Tracer cutting* and *incremental cutting* are two very common methods of cam manufacture. Incremental cutting consists of manufacturing the profile by intermittent cuts based on a table with accurate values of angular cam displacement θ (cam blank) and linear displacement $s(\theta)$ of the follower (cutter). This method is used for making master cams or cams in small numbers. In the tracer control cutting method, the cam surface is milled, shaped, or ground, with the cutter or grinder guided continuously by either a master cam or a computer system. This is the best method for producing large numbers of accurate cam profiles.

In the process of cam and follower manufacturing, several surface imperfections may occur, such as errors, waviness, and roughness. These surface irregularities may induce shock, noise, wear, and vibrations of the cam and follower systems. Imperfections of actual profile cannot exceed an accepted level. Therefore, highly accurate inspection equipment is commonly used in production inspection. Actual displacements of the follower are measured as a function of the cam rotation; then the resulting data can be compared with tabulated theoretical values. By application of the method of finite differences (Sec. 40.3.1), these data can be transformed to actual acceleration curves and compared with theoretical ones. There is, however, a drawback in such a method in that it is based on static measurements.

An example of results obtained from a widely used production inspection method is shown in Fig. 40.15 ([40.5]). Line 1 was obtained from some accurate data from a table of θ values and the corresponding $s(\theta)$ values. Next, two boundary curves were obtained from the basis curve by adding and subtracting 10 percent. This was an arbitrary decision, it being assumed that any acceleration curve contained between such boundaries would be satisfactory. These are shown as upper and lower bounds in Fig. 40.15. The main drawback of the method is that only maximum values of actual acceleration diagrams have been taken into account. It is important to realize that waviness of the real acceleration curve may cause more vibration troubles than will single local surpassing of boundary curves.

A much better method is that of measuring the real acceleration of the follower in an actual cam mechanism at the operating speed of the cam by means of high-quality accelerometers and electronic equipment. To illustrate the importance of proper measurements of the cam profile, we show the results of an investigation of

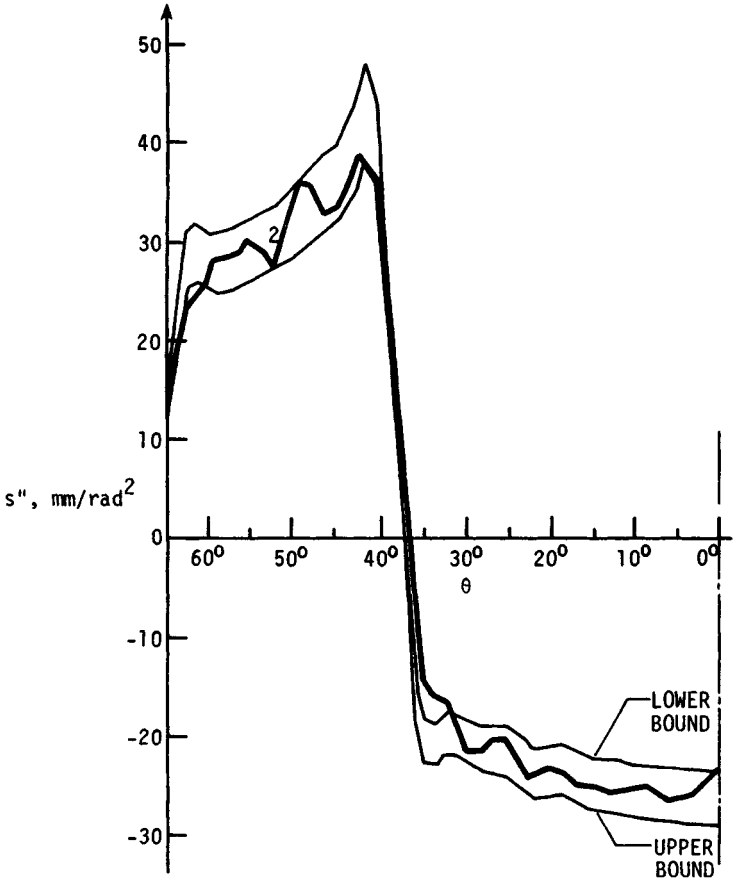

FIGURE 40.15 Example of inspection technique based on acceleration diagram obtained from accurate static measurements of the cam of the Henschel internal combustion engine.

the mechanism used in the Fiat 126 engine ([40.6]). Those results are shown in Figs. 40.16 and 40.17. The acceleration diagram of Fig. 40.16*a* was obtained from designer data by using Eq. (40.29). The diagram plotted as a broken line (1) in Fig. 40.16*b* comes from accurate measurements of a new profile. Here again Eq. (40.29) was applied. The same profile was measured again after 1500 hours (h) of operation, and the acceleration diagram is plotted by a solid line (2) in Fig. 40.16*b*. Comparing curves 1 and 2 of Fig. 40.16*b*, we can see that the wear of the cam smoothed somewhat the waviness of the negative part of the diagram. Accelerations of the follower induced by the same new cam in the actual mechanism (Fig. 40.16*c*) were measured as well by electronic equipment at the design speed, and results of that experiment are presented in Fig. 40.16*d* and *e*. It is obvious from comparison of the diagrams in Fig. 40.16*b* and *d* that the response of the system differs to a considerable extent from the actual input.

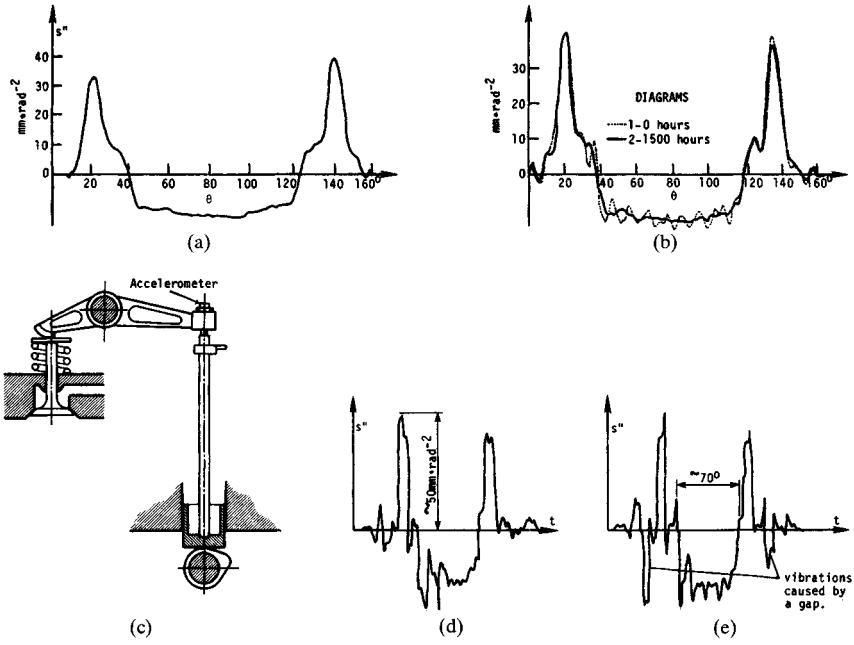

FIGURE 40.16 Comparison between results obtained from static measurements of the Fiat 126 cam profile [(*a*) and (*b*)] and acceleration curves obtained at design speed on the actual engine [(*d*) and (*e*)]. Diagram *d* was obtained for a zero value of backlash and diagram *e* for the factory-recommended 0.2-mm backlash.

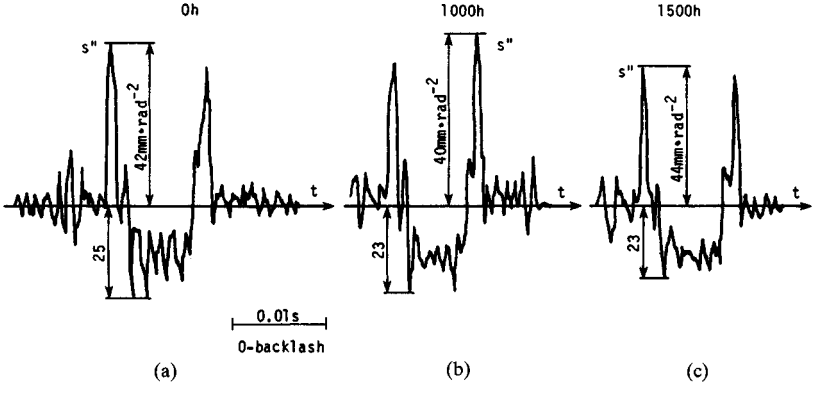

FIGURE 40.17 Changes of acceleration diagram caused by the wear of the cam profile of the Fiat 126.

Eight new cams of the same engine were later used in two separate laboratory stands to find the influence of cam-surface wear on dynamic properties of the cam system. Some of the obtained results are presented in Fig. 40.17. We can observe there that some smoothing of the negative part of the curve (registered as well by statistical measurements) took place after 1500 h. The general character of the acceleration curve remained unchanged, however. (That observation was confirmed later by a Fourier analysis of all the acceleration signals.) The conclusion derived from that single experiment is that dynamic imperfections of the cam system introduced by the process of cam manufacturing may last to the end of the cam life.

40.3.1 Finite-Difference Method

Geometric acceleration of the follower s'' may be estimated by using accurate values of its displacement s from a table of θ versus $s(\theta)$, which comes from the designer's calculations and/or from accurate measurements of the actual cam profile. Denoting as s_{i-1}, s_i, and s_{i+1} three adjacent values of s in such a table, and designating their second finite difference as Δ_i'', we have

$$s_i'' \cong \frac{1}{(\Delta\theta)^2}\Delta_i'' = \frac{s_{i-1} - 2s_i + s_{i+1}}{(\Delta\theta)^2} \tag{40.28}$$

where $\Delta\theta$ = constant increment of the cam's angular displacement θ. A more accurate value of s_i'' can be found from the *average weighted value* (Oderfeld [40.3]) by using entries of 11 adjacent Δ'' from the table of s versus $s(\theta)$:

$$s_i'' = \frac{1}{(\Delta\theta)^2}\sum_{j=-5}^{i=5} W_j\Delta_{i+j}'' \tag{40.29}$$

The weights W_j are given in Table 40.5.

TABLE 40.5 Weights Used in the Improved Finite-Difference Method

j	0	±1	2	±3	±4	±5
W_j	0.31	0.25	0.13	0.015	−0.025	−0.025

An example of an acceleration diagram $s''(\theta)$ of a certain cam obtained using the finite-difference method is presented in Fig. 40.18.

40.4 FORCE AND TORQUE ANALYSIS

A typical approach to dynamic analysis of a rigid cam system can be illustrated by an example of a mechanism with a reciprocating roller follower.† A schematic drawing of such a mechanism is depicted in Fig. 40.19*a*. For the upward motion of the fol-

† Suggestion of Professor Charles R. Mischke, Iowa State University.

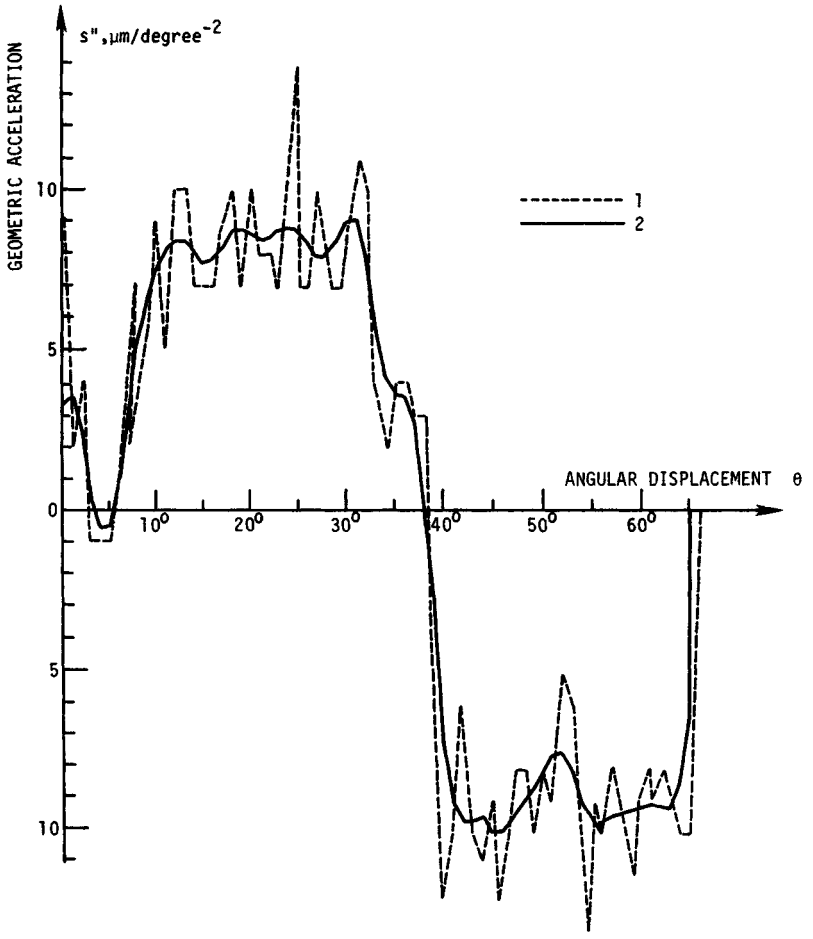

FIGURE 40.18 Acceleration diagrams obtained in the static way. Curve 1 is from Eq. (40.28), curve 2 from Eq. (40.29).

lower, we assume that the follower's stem 4 contacts its guideway at points B and C. As a result of its upward motion, the Coulomb friction at B and C is fully developed and $\tan \psi = \mu$. The free-body diagram of links 3 and 4 is shown in Fig. 40.19*b*. The cam force F_{23} can be resolved into two components: P_{cr} in the critical-angle (γ_{cr}) direction to sustain motion against friction, and P_y in the y direction to produce accelerated motion or to oppose other forces.

It can be found from the geometry of the follower that

$$\gamma_{cr} = \frac{\pi}{2} - \tan^{-1} \mu \left(\frac{2a - \mu d}{l} - \frac{2s}{l} - 1 \right) \tag{40.30}$$

where $a = l_B - R_0 - R_r$. For $\gamma > \gamma_{cr}$, the cam-follower system is self-locking, and motion is impossible. From the force triangle in Fig. 40.19*b* and the rule of sines,

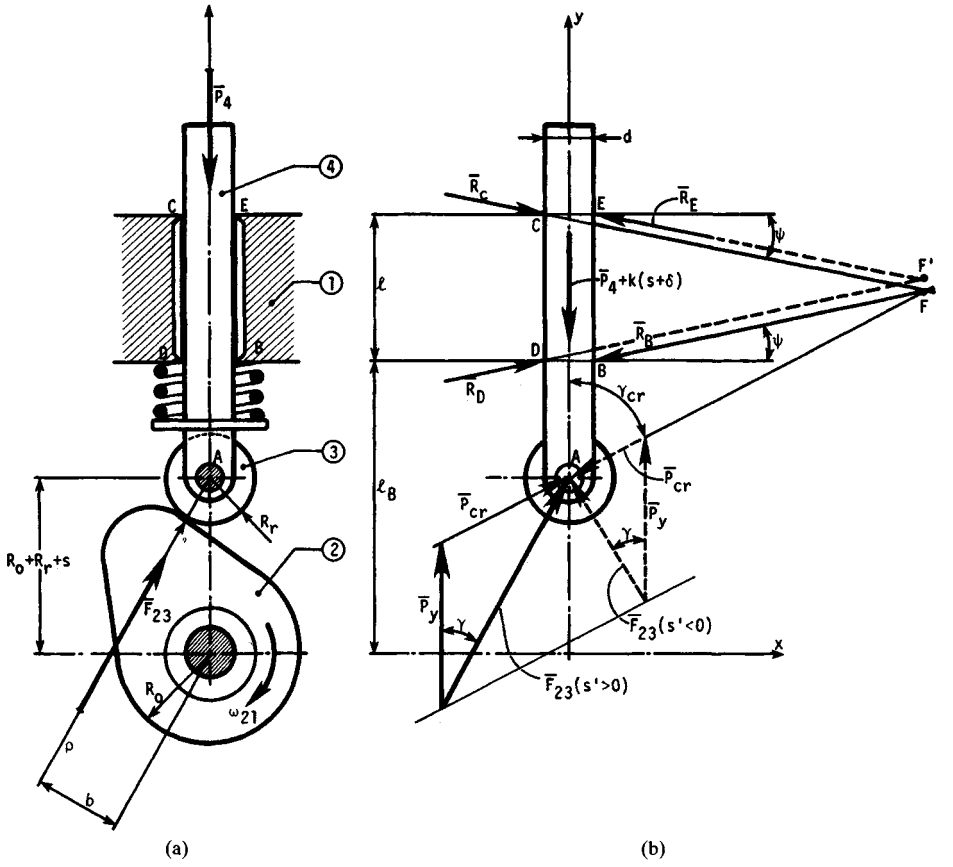

FIGURE 40.19 Force analysis of reciprocating roller-follower cam system.

$$P_y = F_{23}\frac{\sin(\gamma_{cr}-\gamma)}{\sin\gamma_{cr}} \tag{40.31}$$

After finding the vertical component P_y for constant ω_{21} from the force-equilibrium equation, substituting into Eq. (40.31), and solving for F_{23}, we have

$$F_{23} = \frac{\sin\gamma_{cr}(m\omega_{21}^2 s'' + ks + P_4')}{\sin(\gamma_{cr}-\gamma)} \tag{40.32}$$

where m = mass of follower
k = spring rate of retaining spring
$P_4' = P_4 + k\delta$
δ = preset of spring
$k\delta = P_0$; this force is called *preload* of spring

For $F_{23} = 0$, roller and cam lose their contact. The result is called *jump* ([40.7], [40.8]). Assuming $F_{23} = 0$, we can find the jump speed of the cam from Eq. (40.31). The jump occurs for the upward movement of the follower at

$$\omega_{21} \geq \sqrt{\frac{-ks - P_4'}{ms''}} \tag{40.33}$$

Since s is always positive, jump may occur only for negative values of s''. To prevent jump, we increase preload P_0 or the spring rate or both. The driving torque is

$$T_{12} = \frac{\sin \gamma_{cr} \sin \gamma}{\sin (\gamma_{cr} - \gamma)} (R_0 + R_r + s)(m\omega_{21}^2 s'' + ks + P_4') \tag{40.34}$$

We recall that according to Eq. (40.25),

$$\gamma = \tan^{-1} \frac{s'}{s + R_0 + R_r} \tag{40.35}$$

When motion is downward, the contact point of mating surfaces goes to the right side of the roller, cam force F_{23} changes inclination, and new contact points D and E in the follower's guideway replace old ones (B and C, respectively). The new point of concurrency is now at F'. Since in most practical cases points F and F' almost coincide, we can assume that both the point of concurrency and the line of action of force P_{cr} are unchanged. A new vector P_{cr} (broken line) is rotated by 180° with respect to the old one. It is easy to see in Fig. 40.19*b* that F_{23} for downward motion, when γ and P_y equal those for the upward motion, is always smaller than F_{23} for upward motion.

40.4.1 Springs

In cam-follower systems, the follower must contact the cam at all times. This is accomplished by a positive drive or a retaining spring. Spring forces should always prevent the previously described jump of the follower for all the operating speeds of the cam. Thus the necessary preload P_0 of the spring and its spring rate k should be chosen for the highest possible velocity of the cam. By plotting inertial and spring forces, we can find values of preload P_0 and spring rate k that will ensure sufficient load margin for the total range of the follower displacement. We use here only the negative portion of the acceleration curve. Since the follower must be held in contact with the cam, even while operating the system with temporary absence of applied forces, that part of the cam-system synthesis may be accomplished without applied forces. At the critical location, where both curves are in closest proximity, the spring force should exceed the inertial force with friction corrections included by not less than 25 to 50 percent.

40.5 CONTACT STRESS AND WEAR: PROGRAMMING

Let us consider the general case of two cylinderlike surfaces in contact. They are represented by a cam and a follower. The radius of curvature of the follower ρ_1 is equal to the radius of the roller R_r for the roller follower, and it goes to infinity for a flat

follower. The radius of the cam's curvature ρ_2 can be found from the following equation [compare to Eq. (40.23)]:

$$\rho_2 = R_0 + s'' + s \tag{40.36}$$

Equating $d\rho_2/d\theta = s''' + s'$ to zero, we can find the position of the cam, where a minimum of ρ_2 occurs, and find its value from Eq. (40.36). Assuming perfect alignment of the contacting bodies, we have conditions described by Hertz and can check maximum compressive stress σ_c from his well-known equation

$$\sigma_c = 0.558 \sqrt{\frac{P(1/\rho_1 + 1/\rho_2)}{L[(1-\mu_1^2)/E_1 + (1-\mu_2^2)/E_2]}} \tag{40.37}$$

where P = normal load between cam and follower
L = actual thickness of contacting follower and cam
μ_1, μ_2 = Poisson's ratios for follower and cam, respectively
E_1, E_2 = moduli of elasticity of follower and cam, respectively

Some selected data concerning properties of materials for cams and followers are given in [40.7].

Equation (40.37) may be used for finding the minimum permissible value ρ_{min} of the cam's profile radius of curvature. We recall that ρ_{min} was necessary for calculating the values of R_0 and R_r from Eqs. (40.23) and (40.26), respectively.

Rearranging Eq. (40.37) gives, for a roller follower,

$$\rho_{min} \geq \left[3.2\, S_c^2 \frac{L}{P}\left(\frac{1-\mu_1^2}{E_1} + \frac{1-\mu_2^2}{E_2}\right) - \frac{1}{R_r}\right]^{-1} \tag{40.38}$$

The same equation holds true for a flat-faced follower, where $1/R_r = 0$.

Using Eq. (40.38), we can easily check to see if the commonly recommended and used value $\rho_{min} = 0.25$ in (6 mm) is justified in the particular design.

Elements of a cam system, as well as of other machine parts, are subject to wear. The proper choice of metal combinations may increase the life of kinematic pairs of the cam system and decrease their wear. Some experience is necessary in choosing materials to fulfill the requirements of satisfactory cam action with low wear over a long period. Designers, as a rule, prefer to make the follower of softer or first-worn-out material, since manufacturing of the follower is less expensive than manufacturing of the cam profile. There are, however, cases where the cam is cheaper and thus is made of softer material.

40.5.1 Programming of Cam Systems

The steps shown in Fig. 40.20 are as follows:

1. Make a preliminary sketch of your cam system, and estimate the dynamic factor $\mu_d = m_e\omega_c^2/k_e$, according to Eq. (40.8).
2. If your system is a positive drive, go to step 3; otherwise go to step 4.
3. Choose a proper symmetric diagram $s''(\theta)$, and write equations for $s''(\theta)$, $s'(\theta)$, and $s(\theta)$. Write a computer program for θ and $s(\theta)$ with increments of θ equal to 1°.
4. Choose a proper unsymmetric diagram $s''(\theta)$, and proceed as in step 3.
5. Print table of θ and $s(\theta)$.

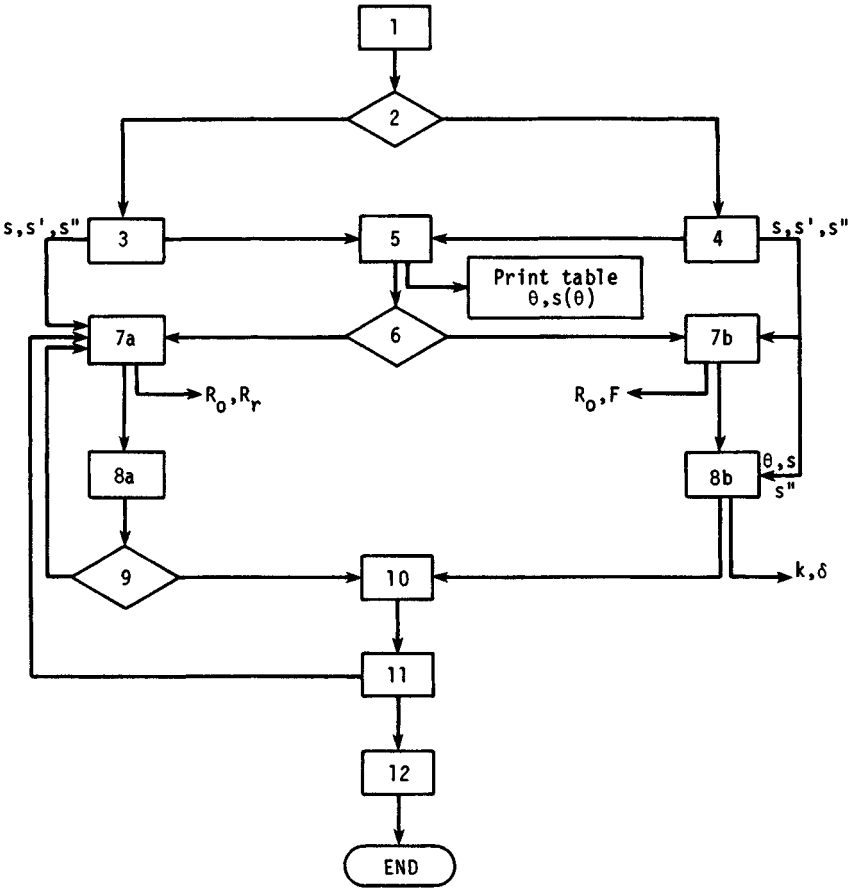

FIGURE 40.20 Programming of cam systems.

6. If you decided to use a roller follower, go to step 7*a;* otherwise go to step 7*b.*
7. *a.* Establish the radius of the roller R_r and the value of maximum pressure angle γ_{max} ($\gamma_{max} \leq 30°$ for the reciprocating follower and $\gamma_{max} \leq 40°$ for the oscillating one). Find the value of θ for which $s'/\tan \gamma_{max} - s - R_r$ is maximum, by equating $s''/\tan \gamma_{max} - s'$ to zero. Calculate the value of the radius R_0 of the prime circle from Eq. (40.26). Go to step 8*a.*

   b. Find the value of θ for which $\rho_{min} - s'' - s$ is maximum, by setting $-(s''' + s')$ to zero. Calculate the value of the radius R_0 of the prime circle from Eq. (40.23). Calculate the face width F from Eq. (40.24). Go to step 8*b.*
8. *a.* Check undercutting of the cam profile from Eq. (40.27).

   b. Find the spring rate of the retaining spring. Go to step 10.
9. If the assumed value R_r is satisfactory, go to step 10; otherwise, assume a new value of R_r and return to step 7*a.*

10. Draw a final version of your cam system (a complete drawing).

11. Write equations describing all the forces in the kinematic pairs, and check the maximum stresses. Find the values of γ_{max} and ρ_{min} for your particular design (if you have a roller follower), and determine whether the actual values of γ and ρ in your design are far enough from γ_{max} and ρ_{min}, respectively; otherwise, return to step 7*a*.

12. Make final corrections in your design.

13. END.

REFERENCES

40.1 M. P. Koster, *Vibrations of Cam Mechanisms,* Philips Technical Library, Macmillan Press, London, 1974.

40.2 C. R. Mischke, *Mathematical Model Building,* Iowa State University Press, Ames, 1980, pp. 316–322.

40.3 J. Oderfeld, "On Application of the Finite-Difference Method for Kinematics of Mechanisms," *Zastosowania Matematyki IV* (in Polish), 1958, pp. 176–195.

40.4 A. A. Olędzki, "Cam Mechanisms," *Wydawnictwa NaukowoTechniczne* (in Polish), Warsaw, Poland, 1966.

40.5 A. A. Olędzki, M. Krawczyński, I. Siwicki, and F. Źrudelny, "On the Automation of Cam-Profile Control," *IFAC Manufacturing Technology Symposium,* Tokyo, 1977.

40.6 A. A. Olędzki and T. Klimowicz, "An Experimental Attempt to Find the Influence of Cam-Profile Wear on the Kinematics of the Cam-Mechanism," *Archiwum Budowy Maszyn* (in Polish), 1979.

40.7 H. A. Rothbart, *Cams—Design, Dynamics, and Accuracy,* John Wiley & Sons, New York, 1956.

40.8 J. E. Shigley and J. J. Uicker, *Theory of Machines and Mechanisms,* 2d ed., McGraw-Hill, New York, 1995.

40.9 D. A. Stoddart, "Polydyne Cam Design," *Machine Design,* January 1953, p. 124; February 1953, p. 146; March 1953, p. 149.

40.10 D. Tesar and G. K. Matthew, *The Dynamic Synthesis, Analysis, and Design of Modeled Cam Systems,* D. C. Heath, Lexington, Mass., 1976.